UDE-Based Robust Droop Control of Inverters in Parallel Operation

Article *in* IEEE Transactions on Industrial Electronics · March 2017

DOI: 10.1109/TIE.2017.2677309

3 authors:

Qing-Chang Zhong
Illinois Institute of Technology
222 PUBLICATIONS **3,362** CITATIONS

SEE PROFILE

Yeqin Wang
Texas Tech University
14 PUBLICATIONS **10** CITATIONS

SEE PROFILE

Beibei Ren
Texas Tech University
53 PUBLICATIONS **1,104** CITATIONS

SEE PROFILE

UDE-Based Robust Droop Control of Inverters in Parallel Operation

Qing-Chang Zhong, *Fellow, IEEE,* Yeqin Wang, *Student Member, IEEE,* and Beibei Ren, *Member, IEEE*

***Abstract*—Conventional droop control methods cannot achieve accurate proportional reactive power sharing, due to the mismatch of components, system disturbances, etc. In this paper, an uncertainty and disturbance estimator (UDE)-based robust droop controller is proposed to address these problems. As a result, the model nonlinearity and uncertainty (e.g., power angle, and uncertain output impedance), and system disturbances (e.g., variations of output impedance, load change, and fluctuating DC-link voltage), can be estimated and compensated. Experimental results from a single-phase system with two inverters are provided to demonstrate the effectiveness of the proposed strategy. In order to further demonstrate the advantage and flexibility of the proposed UDE-based control strategy, simulation results from a three-phase system with two inverters are presented with comparison to a robust droop control strategy reported.**

***Index Terms*—Droop control, uncertainty and disturbance estimator (UDE), robust control, inverters in parallel operation, proportional load sharing.**

I. Introduction

RENEWABLE energies and distributed generations, such as wind energy, solar energy, wave and tidal energy, are growing fast nowadays. Normally, power inverters are adopted in these applications to interface with the utility-grid or the microgrid. However, with the growing capacity of renewable energies, such as MW-level wind turbines, and large-scale solar farms, the power electronic devices face big challenges with the needs of high current and high power. Then several power inverters are required in parallel operation due to the current limitation or cost limitation of power electronic devices. Another reason for the need of parallel operation of inverters is to provide system redundancy and high reliability from the requirements of critical customers [1]. Power sharing based on droop characteristics is widely used in parallel operation of inverters [2]–[4]. Also, sharing the load among distributed generations is popular for the operation of islanded microgrid [5]–[8]. One major advantage of the droop control is that no external communication mechanism is needed [9], which gives significant flexibility without the interdependency of the local controllers for the balance between power generations and the demands [5]. Another advantage is that the system inherits the "plug and play" feature without changing the control strategies of parallel units [6], [10]. However, the conventional droop control is not able to achieve accurate reactive power sharing among parallel units due to the mismatched output impedance [1], [9], [11]–[13], and presents poor transient performance [5], [6]. Also system disturbances, e.g., large or fast change of the load [5], [6], variations of output impedance [13], [14], and fluctuating DC-link voltage [15], [16], often affect the power sharing performance.

The virtual impedance is a widely used approach to improve power sharing performance among parallel operated inverters [9], [17]. Adding a virtual inductor and estimating the effect of the line impedance are proposed in [10] to improve the sharing performance via changing the droop coefficients. The complex virtual impedance is designed in [11] to minimize the fundamental and harmonic circulating currents. The communication and adaptive virtual impedance are combined to enhance the accuracy of reactive power sharing, and the time delay problem in communication is improved in [18]. An accurate power sharing is realized by regulating the virtual impedance at fundamental positive sequence, fundamental negative sequence, and harmonic frequencies in [19]. However, virtual impedance based methods cannot guarantee voltage regulation [7], and the power sharing performance is affected by the variations of the output filter components [13], [14]. With the introduction of virtual impedance, the output voltages of inverters are sensitive to the harmonic currents [20], and the selection of virtual impedance is analyzed in [20]. Many other methods for sharing the load are proposed, e.g., injecting a harmonic voltage according to the output harmonic current is used for improving the total harmonic current sharing, and power sharing is achieved as well in [21]. A small signal injection method is proposed in [22] to improve the accuracy of the reactive power sharing. A Q-V dot droop control method is proposed in [23] to improve the accuracy of reactive power sharing following the idea of changing the droop coefficients. A virtual flux droop method by drooping the virtual flux instead of the voltage is proposed in [24] to achieve real power and reactive power sharing with low frequency deviation. The voltage droop strategy is redesigned to deal with the mismatched output impedance for power sharing in [25], [26]. Especially, the robust droop controller proposed in [25] introduces an integrator to enhance the robustness of droop control against numerical errors, disturbances, noises, feeder impedance, parameter drifts and component mismatches with accurate proportional load sharing, which has recently

Manuscript received July 23, 2016; revised October 15, 2016; November 25, 2016 and December 28, 2016; accepted January 02, 2017.
Qing-Chang Zhong is with the Department of Electrical and Computer Engineering, Illinois Institute of Technology, Chicago, IL 60616, USA. (email: zhongqc@ieee.org).
Yeqin Wang is with the National Wind Institute, Texas Tech University, Lubbock, TX 79409-1021, USA. (e-mail: yeqin.wang@ttu.edu).
Beibei Ren is with the Department of Mechanical Engineering, Texas Tech University, Lubbock, TX 79409-1021, USA. (e-mail: beibei.ren@ttu.edu).

been proven to be universal for inverters having an output impedance angle within $(-\frac{\pi}{2}, \frac{\pi}{2})$ rad [27].

It is worth noting that the hierarchical droop control is another method and trend to cope with the disadvantages of conventional droop control through communication among parallel operated inverters [5], [6], [9], [12]. In hierarchical control methods, e.g. in [28], [29], the primary control is droop control method, and voltage and frequency deviations are compensated by the secondary control through communication. However, hierarchical droop control also has its own drawbacks, such as cost of communication [6], [25], reliability, location and slow responses [6], [25], [30].

In this paper, a new droop control strategy based on the uncertainty and disturbance estimator (UDE) method is developed for parallel operated inverters to achieve accurate proportional load sharing, particularly for reactive power sharing. Compared with other estimator-based controls for distributed generations, such as, linear state estimation [31], Kalman filter based state estimation [32], and estimator-based voltage-predictive control [33], this UDE-based robust droop controller uses a filter to estimate the system uncertainty and disturbances and compensate them for accurate power sharing among parallel operated inverters. The UDE control algorithm, which is proposed in [34], has been successfully applied to a class of non-affine nonlinear systems [35], variable-speed wind turbine control [36], and many other applications [37]–[39] in recent years. In this paper, for reactive power sharing, the reactive power dynamics is developed from the equation of power delivering passed through a low-pass filter. The load voltage is fed back to generate the reactive power reference for the design of the UDE-based controller, which helps achieve accurate sharing control of reactive power. With the adoption of the UDE-based control method, the reactive power sharing can be achieved in the presence of model nonlinearity and uncertainty (e.g., power angle, and uncertain output impedance) and system disturbances (e.g., variations of output impedance, load change, and fluctuating DC-link voltage). For real power sharing, the conventional droop control method is adopted for the frequency regulation, as it can achieve accurate proportional real power sharing [1], [10], [13]. The effectiveness of the proposed control method is demonstrated through experimental studies on an experimental test rig, which consists of two parallel operated power inverters from Texas Instruments (TI). Also, the comparison with the robust droop controller proposed in [25] is made in a three-phase simulation platform to show the advantages and flexibilities of the proposed UDE-based robust droop control.

The rest of this paper is organized as follows. Section II describes the limitation of the conventional droop control. In Section III, the UDE-based robust droop control is proposed. The effectiveness of the proposed approach is demonstrated through experimental validation in Section IV. A comparison with the robust droop controller is conducted in Section V, with concluding remarks made in Section VI.

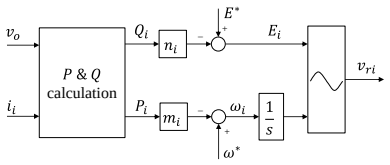

Fig. 1. Conventional droop control scheme.

II. The Limitation of Conventional Droop Control

When a single inverter $E\angle\delta$ delivering power to the grid $V_o\angle 0^\circ$ through an impedance $Z_o\angle\theta$, the real power P and the reactive power Q received by the grid $V_o\angle 0^\circ$ are shown in [1] as

$$P = \left(\frac{EV_o}{Z_o}\cos\delta - \frac{V_o^2}{Z_o}\right)\cos\theta + \frac{EV_o}{Z_o}\sin\delta\sin\theta, \quad (1)$$

$$Q = \left(\frac{EV_o}{Z_o}\cos\delta - \frac{V_o^2}{Z_o}\right)\sin\theta - \frac{EV_o}{Z_o}\sin\delta\cos\theta, \quad (2)$$

where δ is the phase difference between the inverter and the grid, often called the power angle. Usually, the output impedance of an inverter is mostly inductive with $\theta \approx 90^o$. the power delivery equations (1) and (2) are reduced as

$$P = \frac{EV_o}{Z_o}\sin\delta, \quad (3)$$

$$Q = \frac{EV_o}{Z_o}\cos\delta - \frac{V_o^2}{Z_o}. \quad (4)$$

For the conventional droop control [40], power angle δ is assumed to be small. Then,

$$E_i = E^* - n_iQ_i, \quad (5)$$

$$\omega_i = \omega^* - m_iP_i, \quad (6)$$

where E_i is the voltage set-point, ω_i is the frequency set-point, E^* is the rated voltage and ω^* is the rated frequency. n_i and m_i are the droop coefficients, which are related to the capacity of inverters, and usually defined by the requirement of customers. The block diagram of this conventional droop control is shown in Fig. 1.

The limitations of conventional droop control with mismatched output impedance are pointed out in [1]. For example, in order to hold the proportional reactive power sharing

$$n_iQ_i = n_jQ_j, \quad (7)$$

all parallel operated inverters should have the same per-unit output impedance in the steady state

$$\frac{Z_{oi}}{n_i} = \frac{Z_{oj}}{n_j}, \quad (8)$$

where i and j represent all parallel units. This is a very strict condition for inverter design, requiring careful matching of components, for conventional droop control. Moreover, the output impedance of an inverter always drifts in different conditions [13], [14], such as inductance change with magnetic saturation caused by high current, and resistance change by high temperature. Other disadvantages of conventional droop

This article has been accepted for publication in a future issue of this journal, but has not been fully edited. Content may change prior to final publication. Citation information: DOI 10.1109/TIE.2017.2677309, IEEE Transactions on Industrial Electronics

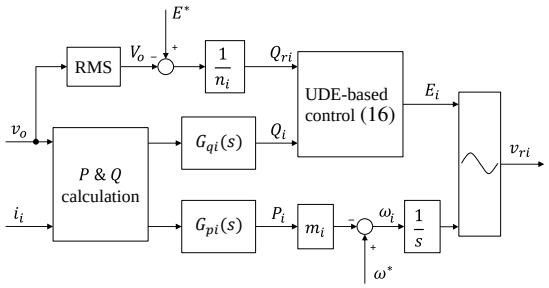

Fig. 2. The proposed UDE-based robust droop control scheme.

control, such as poor transient performance and bad voltage regulation, can be found in [1], [5], [6].

In addition, for the conventional droop control (5) and (6), it is worth noting that the nonlinearity in the equations (1) and (2) of power delivering is approximately linearized based on the assumption that the output impedance of the inverter is purely inductive and the power angle is small. As mentioned before, the system disturbances, e.g. the change of the load, variations of output impedance, and fluctuating DC-link voltage will affect the sharing performance of parallel operated inverters. Is it possible to develop a control strategy that does not rely on these assumptions but can cope with these effects?

III. UDE-Based Robust Droop Control

In this paper, a new droop control scheme is proposed based on the uncertainty and disturbance estimator (UDE) method [34] for parallel operated inverters. Its structure is shown in Fig. 2. For the reactive power sharing, the UDE-based method is adopted to deal with the nonlinearity, uncertainty and system disturbances. For the real power sharing, the conventional droop control method is adopted with the small change of adding a low-pass filter.

A. Reactive Power Sharing

1) Modeling of the Reactive Power Channel: In practice, in order to remove the ripples and high-frequency noises in the calculated real power and reactive power, low-pass filters are commonly adopted when calculating the real power and reactive power. Here, an additional low-pass filter $G_{qi}(s)$ is added to facilitate the controller design. Its bandwidth could be high if the bandwidth of the power calculation is narrow enough. With $G_{qi}(s) = \frac{1}{1+\tau_{qi}s}$, where τ_{qi} is the time constant, the reactive power from (2) can be re-written as

$$Q_i = L^{-1}\left\{\frac{1}{1+\tau_{qi}s}\right\} * \left(\frac{E_i V_o}{Z_{oi}} - \frac{V_o^2}{Z_{oi}} + d_{qi}\right),$$

or,

$$\dot{Q}_i = \frac{E_i V_o}{\tau_{qi} Z_{oi}} - \frac{V_o^2}{\tau_{qi} Z_{oi}} + \frac{d_{qi}}{\tau_{qi}} - \frac{Q_i}{\tau_{qi}}, \tag{9}$$

where "$*$" is the convolution operator, L^{-1} means the inverse Laplace transformation, and

$$\begin{aligned} d_{qi} &= \frac{E_i V_o}{Z_{oi}}(\cos\delta\sin\theta - 1) - \frac{V_o^2}{Z_{oi}}(\sin\theta - 1) \\ &\quad - \frac{E_i V_o}{Z_{oi}}\sin\delta\cos\theta \end{aligned}$$

represents the nonlinearities and uncertainties from both power angle and output impedance. Then the reactive power dynamics can be expressed as

$$\dot{Q}_i = \frac{V_o}{\tau_{qi} Z_{oi}} E_i - \frac{V_o^2}{\tau_{qi} Z_{oi}} + \triangle_{qi}, \tag{10}$$

where

$$\triangle_{qi} = \frac{d_{qi} - Q_i}{\tau_{qi}} \tag{11}$$

represents the lumped uncertain term.

2) Controller Design for Reactive Power Sharing : With the reactive power dynamics developed in (10), a reactive power control is developed for reactive power sharing with the control objective that the output reactive power Q_i asymptotically tracks the reactive power reference Q_{ri}, as shown in Fig. 2. In other words, the tracking error

$$e_{qi} = Q_{ri} - Q_i \tag{12}$$

satisfies the desired dynamic equation

$$\dot{e}_{qi} = -K_{qi} e_{qi}, \tag{13}$$

where $K_{qi} > 0$ is a constant error feedback gain.

Combining (10), (12) and (13), then E_i needs to satisfy

$$E_i = \frac{\tau_{qi} Z_{oi}}{V_o}(\dot{Q}_{ri} + \frac{V_o^2}{\tau_{qi} Z_{oi}} + K_{qi} e_{qi} - \triangle_{qi}). \tag{14}$$

According to the system dynamics in (10), the uncertain term $\triangle_{qi}$ defined in (11) can be represented as

$$\triangle_{qi} = \dot{Q}_i - \frac{V_o}{\tau_{qi} Z_{oi}} E_i + \frac{V_o^2}{\tau_{qi} Z_{oi}}.$$

Following the procedures provided in [34], $\triangle_{qi}$ can be estimated as

$$\begin{aligned} \hat{\triangle}_{qi} &= L^{-1}\{G_{fi}(s)\} * \triangle_{qi} \\ &= L^{-1}\{G_{fi}(s)\} * (\dot{Q}_i - \frac{V_o}{\tau_{qi} Z_{oi}} E_i + \frac{V_o^2}{\tau_{qi} Z_{oi}}), \end{aligned} \tag{15}$$

where $G_{fi}(s)$ is a strictly proper stable filter with the appropriate bandwidth. Replacing $\triangle_{qi}$ with $\hat{\triangle}_{qi}$ in (14) results in

$$\begin{aligned} E_i &= \frac{\tau_{qi} Z_{oi}}{V_o}\Bigg[\dot{Q}_{ri} + \frac{V_o^2}{\tau_{qi} Z_{oi}} + K_{qi} e_{qi} \\ &\quad - L^{-1}\{G_{fi}(s)\} * (\dot{Q}_i - \frac{V_o}{\tau_{qi} Z_{oi}} E_i + \frac{V_o^2}{\tau_{qi} Z_{oi}})\Bigg]. \end{aligned}$$

Then, the UDE-based robust droop control for reactive power sharing can be formulated as

$$\begin{aligned} E_i &= V_o + \frac{\tau_{qi} Z_{oi}}{V_o}\Bigg[L^{-1}\left\{\frac{1}{1 - G_{fi}(s)}\right\} * (\dot{Q}_{ri} + K_{qi} e_{qi}) \\ &\quad - L^{-1}\left\{\frac{s G_{fi}(s)}{1 - G_{fi}(s)}\right\} * Q_i\Bigg]. \end{aligned} \tag{16}$$

Here, V_o appears in the denominator in (16). In practice, when V_o is very small, it would cause a very large E_i and the system might become unstable. This problem can be avoided by setting a minimum value for V_o or replacing V_o in the denominator with the rated voltage.

3) Generation of the Reactive Power Reference: In the aforementioned controller design, the reactive power reference Q_{ri} is needed. Instead of drooping the voltage set-point E_i, the load voltage V_o should be drooped [7], [25], [26]. This idea can be applied to change the voltage droop in (5) as

$$V_o = E^* - n_i Q_{ri}.$$

Then, the reactive power reference can be generated as

$$Q_{ri} = \frac{E^* - V_o}{n_i}, \tag{17}$$

as shown in Fig. 2, where V_o is the root-mean-square (RMS) value of the instantaneous voltage v_o.

It is worth noting that the similar idea of load voltage feedback is adopted in [25], [26] for improving the conventional droop control, via directly re-designing the voltage droop strategy. However, here, the feedback of load voltage is used to generate the reactive power reference, which is different from [25], [26]. With the introduction of load voltage feedback, good regulation of the voltage amplitude can be achieved for the inverters, as validated in Section IV.

B. Stability Analysis

Considering the following Lyapunov function candidate

$$V_Q(t) = \sum n_i^2 Q_i^2,$$

where i =1, 2, ..., N. N is the total number of parallel operated inverters. Taking the derivative of $V_Q(t)$ along with the reactive power dynamics (10) and the UDE-based robust droop control law (16), and combining (12), (15), and (17) lead to

$$\begin{aligned}
\dot{V}_Q(t) &= \sum 2n_i^2 Q_i \dot{Q}_i \\
&= \sum 2n_i^2 Q_i \left(\dot{Q}_{ri} + K_{qi} e_{qi} + \triangle_{qi} - \hat{\triangle}_{qi}\right) \\
&= -\sum 2K_{qi} n_i^2 Q_i^2 + \sum 2n_i^2 Q_i \Bigg(-\frac{\dot{V}_o}{n_i} + \frac{K_{qi} E^*}{n_i} \\
&\quad - \frac{K_{qi} V_o}{n_i} + L^{-1}\left\{1 - G_{fi}(s)\right\} * \triangle_{qi}\Bigg).
\end{aligned}$$

By applying the Young's inequality,

$$\begin{aligned}
\dot{V}_Q(t) &\leq -\sum \left(2K_{qi} - 4\right) n_i^2 Q_i^2 + \sum n_i^2 \Bigg[\left(\frac{\dot{V}_o}{n_i}\right)^2 \\
&\quad + \left(\frac{K_{qi} E^*}{n_i}\right)^2 + \left(\frac{K_{qi} V_o}{n_i}\right)^2 \\
&\quad + \left(L^{-1}\left\{1 - G_{fi}(s)\right\} * \triangle_{qi}\right)^2\Bigg] \\
&\leq -\sum \left(2K_{qi} - 4\right) n_i^2 Q_i^2 + \sum \Bigg[\left(\dot{V}_o\right)^2 \\
&\quad + \left(K_{qi} E^*\right)^2 + \left(K_{qi} V_o\right)^2 + \left(n_i \triangle_{qi}\right)^2\Bigg] \\
&= -\sum \left(2K_{qi} - 4\right) n_i^2 Q_i^2 + \zeta,
\end{aligned} \tag{18}$$

where $\zeta = \sum \left[\left(\dot{V}_o\right)^2 + \left(K_{qi} E^*\right)^2 + \left(K_{qi} V_o\right)^2 + \left(n_i \triangle_{qi}\right)^2\right]$ is a continuous function of Q_1, Q_2, ..., Q_N. On any $\Omega_Q = \left\{(n_1 Q_1, n_2 Q_2, ..., n_N Q_N) \mid V_Q(t) = \sum n_i^2 Q_i^2 < q^2\right\}$ with $q > 0$, ζ has an upper bound $p > 0$, which is a function of q. So,

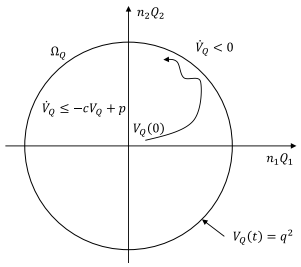

Fig. 3. The invariant set for the stability analysis of two inverters operated in parallel.

$$\dot{V}_Q(t) \leq -cV_Q(t) + p, \tag{19}$$

where $c = \min\{2K_{qi} - 4\} > 0$. If K_{qi} is chosen such that $c > \frac{p}{q^2}$, then $\dot{V}_Q(t) < 0$ when $V_Q(t) \geq q^2$. In other words, the set Ω_Q is an invariant set. Thus, $V_Q(t) < q^2$ for all $t > 0$ if $V_Q(0) = \sum n_i^2 Q_i^2(0) \leq q^2$. An illustration of the set Ω_Q with two parallel operated inverter units is shown in Fig. 3. Therefore, for any $Q_i(0)$, there exist a $K_{qi} > 0$ and a $q > 0$ such that $V_Q(t) < q^2$ or $|Q_i(t)| < \frac{q}{n_i}$. In other words, $Q_i(t)$ is bounded for all $t \geq 0$. Furthermore, V_o and E_i are bounded and currents i_1 and i_2 are bounded too.

In order to analyze the reactive power tracking error e_{qi} of Inverter i, consider the following Lyapunov function candidate

$$V_{ei}(t) = \frac{1}{2} e_{qi}^2.$$

By differentiating $V_{ei}(t)$ with respect to time t, along with the UDE-based control law (16), and combining (15), there is

$$\begin{aligned}
\dot{V}_{ei}(t) &= e_{qi} \dot{e}_{qi} \\
&= -K_{qi} e_{qi}^2 - e_{qi}\left(L^{-1}\left\{1 - G_{fi}(s)\right\} * \triangle_{qi}\right) \\
&= -K_{qi} e_{qi}^2 - e_{qi} \tilde{\triangle}_{qi},
\end{aligned} \tag{20}$$

where $\tilde{\triangle}_{qi} = L^{-1}\left\{1 - G_{fi}(s)\right\} * \triangle_{qi}$ is the estimation error of the uncertain term. By applying the Young's inequality to (20), there is

$$\begin{aligned}
\dot{V}_{ei}(t) &\leq -K_{qi} e_{qi}^2 + \left(\frac{1}{2} e_{qi}^2 + \frac{1}{2} \tilde{\triangle}_{qi}^2\right) \\
&= -\left(K_{qi} - \frac{1}{2}\right) e_{qi}^2 + \frac{1}{2} \tilde{\triangle}_{qi}^2 \\
&\leq -c_1 V_{ei}(t) + c_2,
\end{aligned} \tag{21}$$

where $c_1 = 2K_{qi} - 1$ and $c_2 = \frac{1}{2} \max_t \tilde{\triangle}_{qi}^2$. Then, solving (21) gives

$$0 \leq V_{ei}(t) \leq V_{ei}(0) e^{-c_1 t} + \frac{c_2}{c_1}(1 - e^{-c_1 t}). \tag{22}$$

When $t \to \infty$, $V_{ei}(t) = \frac{1}{2} e_{qi}^2(t)$ is bounded by $\frac{c_2}{c_1} = \frac{\max_t \tilde{\triangle}_{qi}^2}{4K_{qi} - 2}$. In other words, $e_{qi}(\infty) < \frac{\max_t \left|\tilde{\triangle}_{qi}\right|}{\sqrt{2K_{qi} - 1}}$. It can be reduced by increasing the error feedback gain K_{qi} and designing the UDE filter $G_{fi}(s)$ to reduce the maximum estimation error $\max_t \left|\tilde{\triangle}_{qi}\right|$. If the estimation error $\tilde{\triangle}_{qi}$ converges to zero,

then the reactive power tracking error e_{qi} converges to zero too.

C. Performance Analysis of Reactive Power Sharing

With the estimation of uncertain term (15) used in the UDE-based robust droop control (16), the error dynamics (13) of Inverter i becomes

$$\begin{aligned}\dot{e}_{qi} &= -K_{qi}e_{qi} - \left(\triangle_{qi} - \hat{\triangle}_{qi}\right) \\ &= -K_{qi}e_{qi} - L^{-1}\left\{1 - G_{fi}(s)\right\} * \triangle_{qi},\end{aligned}$$

Taking the Laplace transformation,

$$sE_{qi}(s) = -K_{qi}E_{qi}(s) - \blacktriangle_{qi}(s)\left[1 - G_{fi}(s)\right],$$

where $E_{qi}(s)$ and $\blacktriangle_{qi}(s)$ are the Laplace transform of e_{qi} and $\triangle_{qi}$, respectively. Then

$$E_{qi}(s) = -\frac{\blacktriangle_{qi}(s)\left[1 - G_{fi}(s)\right]}{s + K_{qi}}. \tag{23}$$

As discussed before, the uncertain term $\triangle_{qi}$ is bounded. So

$$\lim_{s\to 0} s \cdot \blacktriangle_{qi}(s) < \infty.$$

If the filter $G_{fi}(s)$ is strictly proper and stable with $G_{fi}(0) = 1$, then by applying the final value theorem to (23),

$$\begin{aligned}\lim_{t\to\infty} e_{qi} &= \lim_{s\to 0} s \cdot E_{qi}(s) \\ &= -\lim_{s\to 0} \frac{s \cdot \blacktriangle_{qi}(s)\left[1 - G_{fi}(s)\right]}{s + K_{qi}} \\ &= 0.\end{aligned}$$

Moreover, with the zero reactive power tracking error $e_{qi} = 0$, there is

$$Q_i = Q_{ri} = \frac{E^* - V_0}{n_i}.$$

As a result, the condition for accurate reactive power sharing

$$n_iQ_i = n_jQ_j = E^* - V_0$$

is satisfied because both E^* and V_o are the same for all parallel units. This condition is not affected by the uncertainty in the output impedance, so accurate reactive power sharing can be achieved even when the per-unit output impedance of the inverters are not the same. The uncertainties/variations in output impedance (e.g. caused by parasitic resistance and filter capacitor, by high current, or by high temperature) can be lumped into the uncertain term $\triangle_{qi}$ in (11), which can then be estimated and compensated by the UDE-based control law (16). The load change will affect the power angle, but it can be lumped into the uncertain term $\triangle_{qi}$ in (11), and be compensated. As a result, this UDE-based robust droop control (16) can also handle the disturbance of load change and achieve automatic power balance between the load and inverter units. Furthermore, the variations of the DC-link voltage also can be treated as external disturbances and handled by the proposed method.

Compared with the conventional droop control (5), this UDE-based robust droop control (16) introduces some extra control parameters, error feedback gain in (13) and the UDE filter in (15), to enhance the transient performance of reactive power sharing for parallel operated inverters. In practice, an additional current loop, e.g. in [37], [41], [42], and an additional voltage loop, e.g. in [1], [43], with virtual impedance design can be added into the controller output v_{ri} in Fig. 2 with other purposes, such as improving the voltage quality with less distortion in the output voltage [1], [43], particularly for nonlinear loads, and current protection [1]. In this paper, the impedance deviation of designing virtual impedance can be lumped into the uncertain term $\triangle_{qi}$ in (11), then estimated and compensated by the proposed UDE-based control law (16). Hence, the additional current and voltage loops do not affect the power sharing performance of the proposed method. Since this paper focuses on the robust droop control with uncertainty compensation and disturbance rejection, the virtual impedance design with the voltage loop is not included. The detailed design of the additional voltage and current loops can be found in [1, Chapter 8], with extensive experimental results available in [1, Chapter 20] for various linear and nonlinear loads. The case with a virtual resistor through a current loop is validated in Section IV.

It is worth noting that this method uses local voltage measurement v_o to generate reactive power reference in (17). The same load voltage V_o should be held for accurate reactive power sharing among all parallel units. So this method is suitable for the conditions with small line impedance, such as, power sharing for uninterruptible power supply (UPS) in data centers, MW-level wind turbines or large-scale solar farms. When the line impedance is not negligible, a separate measurement wire can be connected between the inverter terminal and the load terminal to measure the load voltage [25], which provides accurate measurement of the common V_o that is not affected by the line impedance. In this case, the uncertainties/variations in the line impedance can be lumped into uncertain term $\triangle_{qi}$ in (11), which can be estimated and compensated by the proposed UDE-based control law (16). If the line impedance cannot be neglected and separate measurement of the load voltage is not applicable, such as in distributed microgrids, the sharing accuracy will be affected by the line impedances. How to address this problem without involving communication needs some further investigation.

D. Real Power Sharing

The conventional droop control (6) is able to achieve accurate real power sharing [25] when the line impedance is negligible so no major change is needed, apart from adding the first-order low-pass filter

$$G_{pi}(s) = \frac{1}{\tau_{pi}s + 1}.$$

The frequency regulation in (6) can be re-written as

$$m_iP_i = \omega^* - \omega_i.$$

When the system is in the steady state, all parallel operated inverters are working under the same frequency [10], [13]. Then

$$m_iP_i = m_jP_j$$

is easily achieved with the same ω_i for all parallel units, which guarantees accurate real power sharing.

This article has been accepted for publication in a future issue of this journal, but has not been fully edited. Content may change prior to final publication. Citation information: DOI 10.1109/TIE.2017.2677309, IEEE Transactions on Industrial Electronics

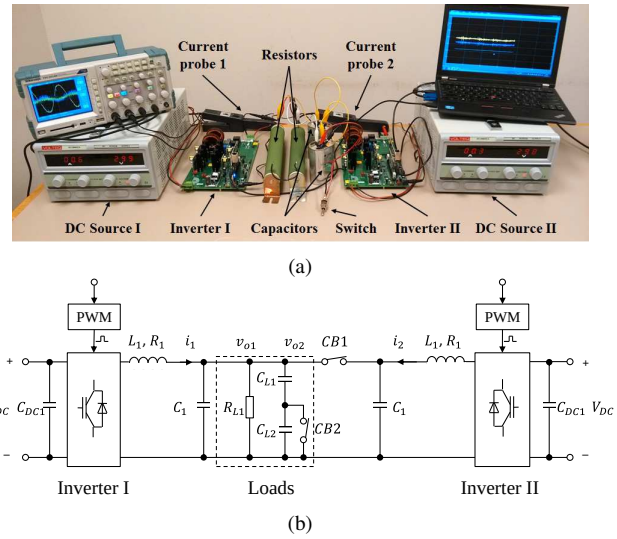

Fig. 4. Experimental test rig: (a) Setup, (b) Circuit diagram.

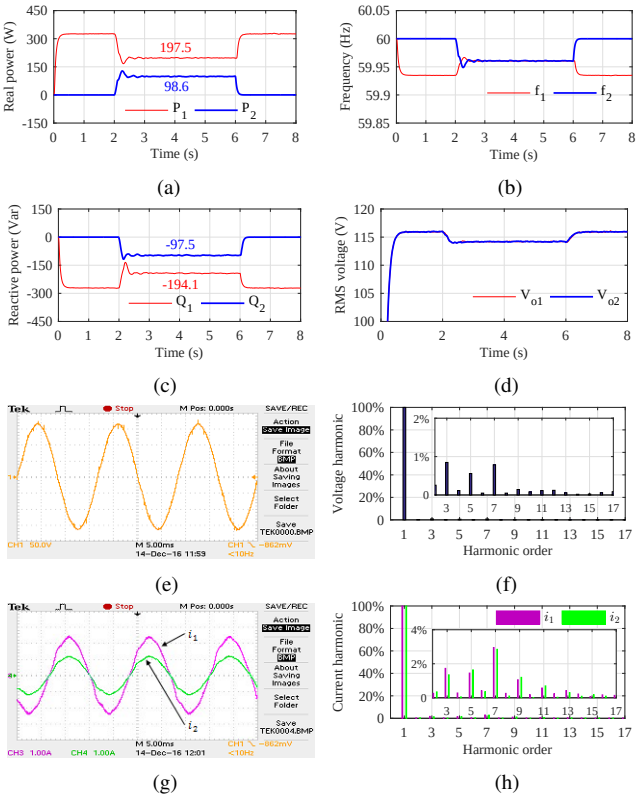

Fig. 5. Nominal experimental results for power sharing performance. (a) Real power, (b) Inverter frequency, (c) Reactive power, (d) RMS voltage, (e) AC voltage v_o, (f) Spectrum of v_o, (g) AC currents, (h) Spectrum of currents.

IV. Experimental Validation

A. Experimental Setup

To verify the effectiveness of the UDE-based robust droop control, a test rig with two single-phase parallel operated inverters, TI TMDSHV1PHINVKITs, as shown in Fig. 4(a) is built up. The circuit diagram is shown in Fig. 4(b), where both inverters are powered by two isolated DC sources. The load consists of a resistor $R_{L1} = 40\ \Omega$ in parallel with two 45 μF capacitors C_{L1} and C_{L2}. The capacitor C_{L2} is initially bypassed by a switch $CB2$. Inverter I is connected to the load directly and Inverter II is connected to the load via a switch $CB1$. In order to synchronize Inverter II to Inverter I, the load voltage v_{o2} is measured by Inverter II. The parameters of the inverters are given in Table I. Here, the output impedance of inverter includes the parasitic resistance. As mentioned before, the effect of resistance also can be lumped into the uncertain term $\triangle_{qi}$ (11) and be compensated in the controller design. The PWM frequency for power electronic devices is set as 19.2 kHz for both inverters. Both inverters are controlled through the TI controlCARD with TI F28M35H52C1 microcontroller (MCU). The measurements and embedded control algorithms are running in the TI MCU. The signals inside the controller, together with the measurements, are sent out through the MCU serial communication port to a desktop for plotting. The load voltage and output currents of both inverters are recorded with an oscilloscope to demonstrate the power sharing performance.

TABLE I
Inverter Parameters.

Parameters	Values	Parameters	Values
L_1	3.5 mH	Nominal V_{DC}	200 V
R_1	0.6 Ω	Rated frequency	60 Hz
C_1	5 μF	Rated voltage	110 V_{rms}
C_{DC1}	560 μF	-	-

The load voltage v_{oi} and output current i_i are measured and sent back to the TI MCU, as shown in Fig. 4(b). The real power P_i and the reactive power Q_i are calculated by taking the average of the instantaneous power over a period $T_i = \frac{2\pi}{\omega_i}$ as

$$P_i = \frac{1}{T_i}\int_{t}^{t+T_i} v_{oi}(\tau)i_i(\tau)d\tau, \quad Q_i = \frac{1}{T_i}\int_{t}^{t+T_i} v_{odi}(\tau)i_i(\tau)d\tau,$$

where v_{odi} is v_{oi} delayed by $\frac{\pi}{2}$ rad. This is equivalent to passing the instantaneous values $v_{oi}(t)i_i(t)$ and $v_{odi}(t)i_i(t)$ through the hold filter $\frac{1-e^{-T_i s}}{T_i s}$ [44], which embeds a low-pass filter effect with a cut-off frequency of $\frac{2/T_i}{2\pi} = \frac{\omega_i}{2\pi^2} \approx 15.9$ Hz. This is much lower than the cut-off frequency of G_{pi} and G_{qi}, i.e., $\frac{1/0.0005}{2\pi} = 318$ Hz, and the grid frequency 60 Hz.

B. Selection of Control Parameters

It is worth noting that the UDE-based control law (16) includes a derivative term $\dot{Q}_{ri}$. According to [45], a low pass filter can be introduced to approximate $\dot{Q}_{ri}$ numerically as

$$\tilde{Q}_{ri} = L^{-1}\left\{\frac{1}{1+\tau_{ri}s}\right\} * Q_{ri},$$

TABLE II
Control Parameters for (24).

Parameters	Values	Parameters	Values
τ_{q1}, τ_{q2}	0.0005 s	K_{q1}, K_{q2}	100
τ_{p1}, τ_{p2}	0.0005 s	τ_1, τ_2	0.004 s
τ_{r1}, τ_{r2}	0.0005 s	-	-

This article has been accepted for publication in a future issue of this journal, but has not been fully edited. Content may change prior to final publication. Citation information: DOI 10.1109/TIE.2017.2677309, IEEE Transactions on Industrial Electronics

from which there is

$$\tau_{ri}\dot{\tilde{Q}}_{ri} + \tilde{Q}_{ri} = Q_{ri}.$$

With the approximation of $\dot{Q}_{ri}$ by $\dot{\tilde{Q}}_{ri}$, the final control law for implementation is derived as

$$\begin{aligned} E_i &= V_o + \frac{\tau_{qi} Z_{oi}}{V_o}\Bigg[L^{-1}\left\{\frac{1}{1-G_{fi}(s)}\right\} \\ &\quad *\left(\frac{Q_{ri}-\tilde{Q}_{ri}}{\tau_{ri}} + K_{qi}e_{qi}\right) \\ &\quad -L^{-1}\left\{\frac{sG_{fi}(s)}{1-G_{fi}(s)}\right\} * Q_i\Bigg]. \end{aligned} \tag{24}$$

In practice, this control law (24) should be simplified to avoid any unstable pole-zero cancellation and then converted into the discrete-time domain for implementation in the TI MCU. Again, the V_o in the denominator should be bounded by a value large enough or be replaced with the rated voltage.

In this paper, the cut-off frequency of the filters $G_{qi}(s)$ and $G_{pi}(s)$ should be small enough in order not to cause any problems in implementation. The cut-off frequency of the low pass filters to approximate $\dot{Q}_{ri}$ can be chosen the same value as $G_{qi}(s)$ and $G_{pi}(s)$. $\frac{1}{K_{qi}}$ is a time constant for the step response of the desired tracking error dynamics (13). The UDE filter $G_{fi}(s)$ is chosen as a first-order low-pass filter $G_{fi}(s) = \frac{1}{1+\tau_i s}$ with the time constant τ_i so that the bandwidth is wide enough to cover the spectrum of $\triangle_{qi}$ in (11) and to achieve fast system response. The control parameters for the control law (24) with $G_{fi}(s) = \frac{1}{1+\tau_i s}$ are shown in Table II.

The capacities of the two inverters are assumed as 0.5 kVA and 0.25 kVA, and the droop coefficients are chosen as $n_1 = 0.022$ and $n_2 = 0.044$; $m_1 = 0.0004\pi$ and $m_2 = 0.0008\pi$. Hence, it is expected that $P_1 = 2P_2$ and $Q_1 = 2Q_2$. The Z_{oi} in the control law (24) implemented is chosen as the nominal value in Table I. Although the same model of inverters with the same nominal output impedance are used, the sharing ratio of 2:1 corresponding to different power capacities is set.

C. System Performance

1) Case 1: nominal case: Initially, the load is connected to Inverter I only, with switch $CB1$ OFF and switch $CB2$ ON. Inverter II is connected to the load at $t = 2$ s by turning switch $CB1$ ON. At $t = 6$ s, Inverter II is disconnected.

The system response curves with the proposed UDE-based robust droop control (16) and (6) are shown in Fig. 5. Initially, only Inverter I is connected to the load. The frequency drop is shown in Fig. 5(b) due to the effect of positive real power as shown in Fig. 5(a). The voltage drop as shown in Fig. 5(d) is high in the single-inverter mode, and the negative drop direction is due to the effect of negative reactive power as shown in Fig. 5(c) with the capacitive load. At $t = 2$ s, switch $CB1$ is turned ON, and Inverter II is connected to the load. The load voltage v_{o2} is measured by Inverter II for voltage synchronization with the zero-crossing method [1]. Some small spikes can be seen in both real power and reactive power at the connecting moment, as the voltages on both sides of switch $CB1$ have little differences before connection. Both real power and reactive power achieve 2:1 sharing very quickly (within about 0.5 s) after $t = 2$ s. It shows that the UDE-based robust droop control can achieve good power sharing performance with the fast response. With the Inverter II connected to the load, the voltage drop is smaller than that in the single-inverter mode, and the output voltage is closer to the rated voltage. So the UDE-based robust droop control has the good voltage regulation capability. The frequencies of both parallel operated inverters are the same in the steady state, and the frequency drop is also smaller in the parallel-operation mode. At $t = 6$ s, Inverter II is disconnected, the reactive power and voltage, real power and frequency of Inverter I are back to the initial state. The AC voltage at about $t = 4$ s is shown in the Fig. 5(e). The spectrum of this recorded voltage is shown in the Fig. 5(f), with the total harmonic distortion (THD) of 1.54%. The AC currents are shown in Fig. 5(g), where the current sharing reflects both real power sharing and reactive power sharing well. The spectra of both recorded currents are shown in Fig. 5(h), with THDs of 4.05% and 4.12%, respectively. It can be seen that the major harmonics are of the 3rd order, the 5th order and the 7th order. The steady state power sharing performance is shown in Table III. According to the formulas proposed in [1] to calculate the sharing errors, the sharing errors for the real power and

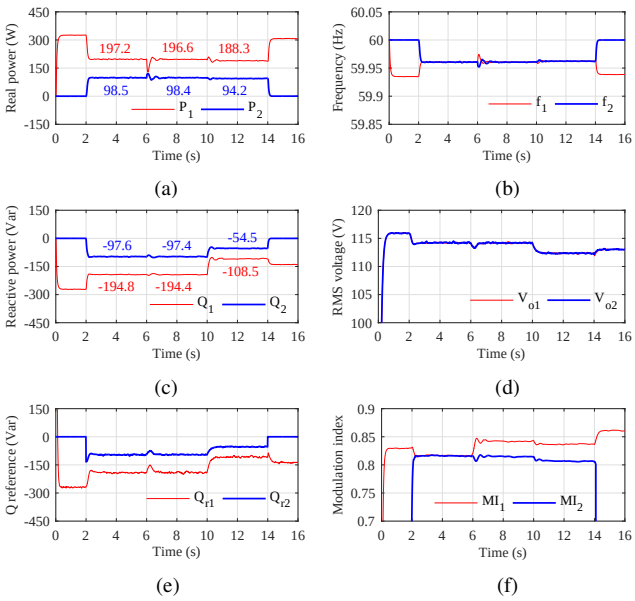

Fig. 6. Transient experimental results with disturbances rejection. (a) Real power, (b) Inverter frequency, (c) Reactive power, (d) RMS voltage, (e) Reactive power reference, (f) Modulation index ($\frac{\sqrt{2}E_i}{V_{DC}}$)

TABLE III
STEADY POWER SHARING PERFORMANCES.

Parameters	Values
Inverter I average apparent power (VA)	197.5-194.1j
Inverter II average apparent power (VA)	98.6-97.5j
P sharing error $\frac{3(P_1-2P_2)}{2(P_1+P_2)} \times 100\%$	0.15%
Q sharing error $\frac{3(Q_1-2Q_2)}{2(Q_1+Q_2)} \times 100\%$	0.46%

This article has been accepted for publication in a future issue of this journal, but has not been fully edited. Content may change prior to final publication. Citation information: DOI 10.1109/TIE.2017.2677309, IEEE Transactions on Industrial Electronics

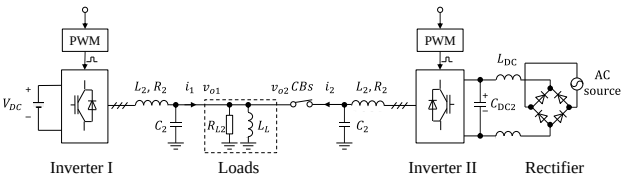

Fig. 7. Three-phase simulation platform

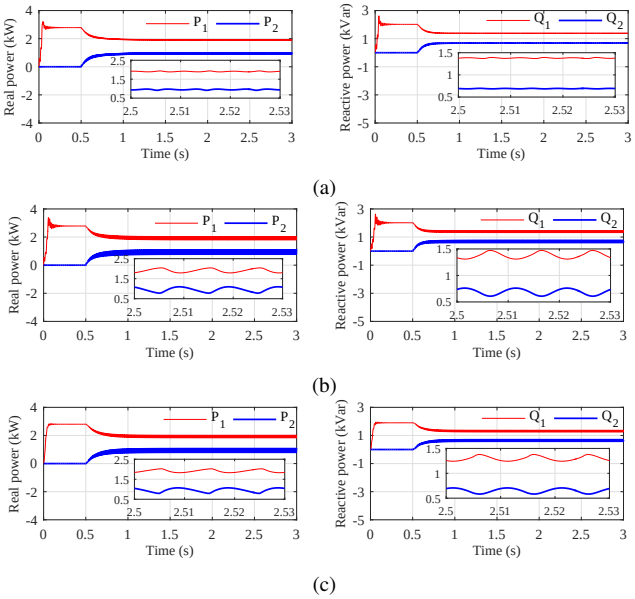

Fig. 8. Comparison of three control methods with both real power (left column) and reactive power (right column). (a) UDE with IMP, (b) UDE without IMP, (c) RDC.

the reactive power are 0.15% and 0.46%, respectively, which indicates that the UDE-based robust droop control can achieve very accurate power sharing.

2) Case 2: disturbance rejection: In this case, two disturbances are considered: change of the output impedance, and change of the load. Initially, the load is connected to the Inverter I only, with switch $CB1$ OFF and switch $CB2$ ON. Inverter II is connected to the load at $t = 2$ s by turning switch $CB1$ ON. At $t = 6$ s, a virtual output impedance $R_{v1} = 2\,\Omega$ with feedback current is added in Inverter I. This virtual output impedance mimics the disturbance from the variation of output impedance. At $t = 10$ s, switch $CB2$ is turned OFF to change the capacitive load from 45 μF to 22.5 μF. At $t = 14$ s, Inverter II is disconnected.

The system responses are shown in the Fig. 6. After $t = 6$ s, there is a negative spike in the real power of Inverter I, as the increase of output impedance reduces power output of inverter I, and the real power of inverter II has a positive spike correspondingly, as shown in Fig. 6(a). The frequency responses are shown in Fig. 6(b). Both real power and frequency settle down quickly within 0.4 s, and real power still keeps 2:1 sharing. The reactive power of both inverters only has very small spikes and still keeps the sharing ratio very well as shown in Fig. 6(c). Also, the reactive power shown in Fig. 6(c) tracks the reactive power reference shown in Fig. 6(e) well. The output voltage has small drop and goes back quickly,

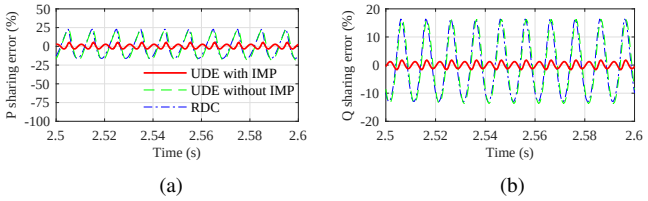

Fig. 9. Power sharing errors of three methods. (a) of real power, (b) of reactive power

TABLE IV
THE RMS OF STEADY STATE POWER SHARING ERROR (2S-3S).

Controllers	UDE with IMP	UDE without IMP	RDC
P sharing error	2.6%	14.3%	14.0%
Q sharing error	1.0%	11.1%	10.3%

as shown in Fig. 6(d). The modulation index of Inverter I increases after adding the virtual output impedance, as shown in Fig. 6(f), while the modulation index of Inverter II remains more or less the same. After $t = 10$ s, the real power and frequency almost remain unchanged as shown in Fig.6(a) and Fig. 6(b), as the resistive load keeps the same. The reactive powers converge to new steady state values in a very short time (within 0.4 s), and the sharing ratio can still maintain at 2:1, as shown in Fig. 6(c). In Fig. 6(d), the output voltage goes down with lower reactive power output. The modulation indexes of both inverters drop a little. At $t = 14$ s, Inverter II is disconnected, the real power and frequency of Inverter I are almost back to initial state, while the reactive power is about half of the initial value due to the half capacitive load. The voltage is lower than the initial value due to the lower reactive power output. The modulation index of Inverter I is much bigger than its initial value, due to the added virtual output impedance with a high output current.The experimental results indicate that the UDE-based robust droop control can effectively reject the disturbance from variations of the output impedance and has good robustness against the load change.

V. COMPARISON WITH THE ROBUST DROOP CONTROLLER

To further demonstrate the advantage and flexibility of the proposed UDE-based robust droop control, the UDE filter is redesigned to handle periodical disturbances, e.g. those caused by fluctuating DC-link voltages, or three-phase unbalanced loads. Its performance is compared with the robust droop controller (RDC) proposed in [25], because the RDC is able to regulate the voltage and has good performance and robustness against different kinds of uncertainties and disturbances.

In this case, a three-phase simulation platform with two inverters, as shown in Fig. 7, is built in MATLAB/Simulink/SimPowerSystems. Inverter I is powered by a normal DC source with $V_{\rm DC} = 600$ V and Inverter II is powered by a single-phase AC source (380 $V_{\rm rms}$, 50 Hz) with a diode rectifier with an LC filter $L_{\rm DC} = 100$ μH, $C_{\rm DC2} = 800$ μF. The inverter parameters are $L_2 = 4.4$ mH, $R_2 = 1.0$ Ω, and $C_2 = 10\,\mu$F [46], [47]. The load is a three-phase RL load with $R_{L2} = 12$ Ω and $L_L = 47$ mH. The DC-link voltage

of the capacitor $C_{\rm DC2}$ fluctuates at 100 Hz due to the single-phase rectifier. The rated phase voltage is still 110 $V_{\rm rms}$ and 60 Hz in this three-phase system.

The UDE filter G_{f1} for Inverter I is still chosen as a first-order low-pass filter with $G_{f1}(s) = \frac{1}{1+\tau_1 s}$, while G_{f2} for Inverter II is designed as

$$G_{f2}(s) = 1-(1-\frac{1}{1+\tau_2 s})(1-\frac{\frac{\omega_0}{Q_{q2}}s}{s^2+\frac{\omega_0}{Q_{q2}}s+\omega_0^2}\cdot \text{SW}), \quad (25)$$

where $\frac{1}{1+\tau_2 s}$ is a first-order filter to handle step responses or step disturbances, $\frac{\frac{\omega_0}{Q_{q2}}s}{s^2+\frac{\omega_0}{Q_{q2}}s+\omega_0^2}$ is a second-order bandpass filter based on the internal model principle (IMP) [48]–[50] to handle the sinusoidal disturbance with the frequency ω_0. SW={0, 1} is a digital switch to switch ON/OFF the filter design with IMP, according to different application scenarios. When SW=0, the $G_{f2}(s)$ is a first-order low-pass filter .

Three controllers are studied in this case: UDE-based control (16) with $G_{f2}(s)$ in (25) and SW=1 (UDE with IMP), UDE-based control (16) with $G_{f2}(s)$ in (25) and SW=0 (UDE without IMP), and RDC in [25]. For UDE-based control with IMP, the parameters are set as $\omega_0 = 200\pi$, $Q_{q2} = 0.2$ to deal with 100 Hz periodical fluctuations in the DC-link voltage. For the RDC in [25], the parameter K_e is set as 30. The droop coefficients are chosen as $n_1 = 0.0022$ and $n_2 = 0.0044$; $m_1 = 0.00004\pi$ and $m_2 = 0.00008\pi$. Other control parameters are the same as those in the experimental case as shown in Table II. Here, the real power P_i and reactive power Q_i are calculated via the instantaneous power in a three-phase system.

The simulation results from the three controllers are shown in Fig. 8. The three methods have similar transient performance when Inverter II is connected to the system with CBs ON. Both real power and reactive power settle down quickly within about 0.25 s. The UDE-based control with IMP has better performance than UDE without IMP and RDC to handle the disturbance of 100 Hz periodical fluctuation in DC-link voltage, with much smaller fluctuations of both real power and reactive power in both inverters, as shown in Fig. 8. The RMS of the steady state power sharing errors (during 2 s to 3 s) are only 2.6% for real power and 1.0% for reactive power with the UDE-based control with IMP, which are much smaller than that of the UDE without IMP, 14.3% for real power and 11.1% for reactive power, and that of RDC, 14.0% for real power and 10.3% for reactive power, as shown in Table IV. The related power sharing errors are plotted in Fig. 9 within 2.5 s to 2.6 s. Therefore, the UDE-based control is very flexible in designing the filter according to different application scenarios. The UDE-based robust droop control with IMP has better performance than the RDC proposed in [25] in handling periodical disturbances.

VI. Conclusion

In this paper, an UDE-based robust droop controller has been proposed for accurate proportional load sharing among parallel operated inverters. For the reactive power sharing, the UDE-based droop method has been adopted to deal with the model nonlinearity and uncertainty (e.g., power angle, and uncertain output impedance), and system disturbances (e.g., variations of output impedance, load change, and fluctuating DC-link voltage). For the real power sharing, the conventional droop method has been applied with the small change of adding a low-pass filter. The theoretical analysis for power sharing has been investigated. The effectiveness of the proposed UDE-based robust droop controller has been validated by both simulation studies and experimental validation.

Acknowledgment

The authors would like to thank the Reviewers and the Editors for their constructive comments and suggestions, which have improved the quality of this paper, and also would like to thank Texas Instruments for the donation of inverter kit TMDSHV1PHINVKIT.

References

[1] Q.-C. Zhong and T. Hornik, *Control of Power Inverters in Renewable Energy and Smart Grid Integration*. Wiley-IEEE Press, 2013.

[2] J. M. Guerrero, M. Chandorkar, T. Lee, and P. Loh, "Advanced control architectures for intelligent microgrids-Part I: Decentralized and hierarchical control," *IEEE Trans. Ind. Electron.*, vol. 60, no. 4, pp. 1254–1262, Apr. 2013.

[3] S. M. Ashabani and Y. A. I. Mohamed, "A flexible control strategy for grid-connected and islanded microgrids with enhanced stability using nonlinear microgrid stabilizer," *IEEE Trans. Smart Grid*, vol. 3, no. 3, pp. 1291–1301, Sept. 2012.

[4] Y. Guan, J. M. Guerrero, X. Zhao, J. C. Vasquez, and X. Guo, "A new way of controlling parallel-connected inverters by using synchronous-reference-frame virtual impedance loop–Part I: Control principle," *IEEE Trans. Power Electron.*, vol. 31, no. 6, pp. 4576–4593, Jun. 2016.

[5] D. E. Olivares, A. Mehrizi-Sani, A. H. Etemadi, C. A. Canizares, R. Iravani, M. Kazerani, A. H. Hajimiragha, O. Gomis-Bellmunt, M. Saeedifard, R. Palma-Behnke, G. A. Jimenez-Estevez, and N. D. Hatziargyriou, "Trends in microgrid control," *IEEE Trans. Smart Grid*, vol. 5, no. 4, pp. 1905–1919, Jul. 2014.

[6] M. Yazdanian and A. Mehrizi-Sani, "Distributed control techniques in microgrids," *IEEE Trans. Smart Grid*, vol. 5, no. 6, pp. 2901–2909, Nov. 2014.

[7] H. Han, X. Hou, J. Yang, J. Wu, M. Su, and J. M. Guerrero, "Review of power sharing control strategies for islanding operation of AC microgrids," *IEEE Trans. Smart Grid*, vol. 7, no. 1, pp. 200–215, Jan. 2016.

[8] A. Milczarek, M. Malinowski, and J. M. Guerrero, "Reactive power management in islanded microgrid-proportional power sharing in hierarchical droop control," *IEEE Trans. Smart Grid*, vol. 6, no. 4, pp. 1631–1638, Jul. 2015.

[9] J. M. Guerrero, L. Hang, and J. Uceda, "Control of distributed uninterruptible power supply systems," *IEEE Trans. Ind. Electron.*, vol. 55, no. 8, pp. 2845–2859, Aug. 2008.

[10] Y. Li and C.-N. Kao, "An accurate power control strategy for power-electronics-interfaced distributed generation units operating in a low-voltage multibus microgrid," *IEEE Trans. Power Electron.*, vol. 24, no. 12, pp. 2977–2988, Dec. 2009.

[11] W. Yao, M. Chen, J. Matas, J. M. Guerrero, and Z.-M. Qian, "Design and analysis of the droop control method for parallel inverters considering the impact of the complex impedance on the power sharing," *IEEE Trans. Ind. Electron.*, vol. 58, no. 2, pp. 576–588, Feb. 2011.

[12] J. M. Guerrero, J. C. Vasquez, J. Matas, L. G. de Vicuna, and M. Castilla, "Hierarchical control of droop-controlled AC and DC microgrids-a general approach toward standardization," *IEEE Trans. Ind. Electron.*, vol. 58, no. 1, pp. 158–172, Jan. 2011.

[13] A. Micallef, M. Apap, C. S. Staines, J. M. Guerrero, and J. C. Vasquez, "Reactive power sharing and voltage harmonic distortion compensation of droop controlled single phase islanded microgrids," *IEEE Trans. Smart Grid*, vol. 5, no. 3, pp. 1149–1158, May 2014.

[14] T.-F. Wu, C.-H. Chang, L.-C. Lin, G.-R. Yu, and Y.-R. Chang, "A D-Σ digital control for three-phase inverter to achieve active and reactive power injection," *IEEE Trans. Ind. Electron.*, vol. 61, no. 8, pp. 3879–3890, Aug. 2014.

[15] X. Yuan, F. Wang, D. Boroyevich, Y. Li, and R. Burgos, "DC-link voltage control of a full power converter for wind generator operating in weak-grid systems," *IEEE Trans. Power Electron.*, vol. 24, no. 9, pp. 2178–2192, Sept. 2009.

[16] M. Ashabani and Y. A.-R. I. Mohamed, "Novel comprehensive control framework for incorporating VSCs to smart power grids using bidirectional synchronous-VSC," *IEEE Trans. Power Syst.*, vol. 29, no. 2, pp. 943–957, Mar. 2014.

[17] X. Wang, Y.-W. Li, F. Blaabjerg, and P. C. Loh, "Virtual-impedance-based control for voltage-source and current-source converters," *IEEE Trans. Power Electron.*, vol. 30, no. 12, pp. 7019–7037, Dec. 2015.

[18] H. Mahmood, D. Michaelson, and J. Jiang, "Accurate reactive power sharing in an islanded microgrid using adaptive virtual impedances," *IEEE Trans. Power Electron.*, vol. 30, no. 3, pp. 1605–1617, Mar. 2015.

[19] J. He, Y.-W. Li, and F. Blaabjerg, "An enhanced islanding microgrid reactive power, imbalance power, and harmonic power sharing scheme," *IEEE Trans. Power Electron.*, vol. 30, no. 6, pp. 3389–3401, Jun. 2015.

[20] W. Wang, X. Zeng, X. Tang, and C. Tang, "Analysis of microgrid inverter droop controller with virtual output impedance under non-linear load condition," *IET Proc. Power Electron.*, vol. 7, no. 6, pp. 1547–1556, Jun. 2014.

[21] U. Borup, F. Blaabjerg, and P. Enjeti, "Sharing of nonlinear load in parallel-connected three-phase converters," *IEEE Trans. Ind. Appl.*, vol. 37, no. 6, pp. 1817–1823, Nov./Dec. 2001.

[22] A. Tuladhar, H. Jin, T. Unger, and K. Mauch, "Control of parallel inverters in distributed AC power systems with consideration of line impedance effect," *IEEE Trans. Ind. Appl.*, vol. 36, no. 1, pp. 131–138, Jan./Feb. 2000.

[23] C.-T. Lee, C.-C. Chu, and P.-T. Cheng, "A new droop control method for the autonomous operation of distributed energy resource interface converters," *IEEE Trans. Power Electron.*, vol. 28, no. 4, pp. 1980–1993, Apr. 2013.

[24] J. Hu, J. Zhu, D. G. Dorrell, and J. M. Guerrero, "Virtual flux droop method-a new control strategy of inverters in microgrids," *IEEE Trans. Power Electron.*, vol. 29, no. 9, pp. 4704–4711, Sept. 2014.

[25] Q.-C. Zhong, "Robust droop controller for accurate proportional load sharing among inverters operated in parallel," *IEEE Trans. Ind. Electron.*, vol. 60, no. 4, pp. 1281–1290, Apr. 2013.

[26] C. Sao and P. Lehn, "Autonomous load sharing of voltage source converters," *IEEE Trans. Power Del.*, vol. 20, no. 2, pp. 1009–1016, Apr. 2005.

[27] Q.-C. Zhong and Y. Zeng, "Universal droop control of inverters with different types of output impedance," *IEEE Access*, vol. 4, pp. 702–712, Jan. 2016.

[28] S. Liu, X. Wang, and P.-X. Liu, "Impact of communication delays on secondary frequency control in an islanded microgrid," *IEEE Trans. Ind. Electron.*, vol. 62, no. 4, pp. 2021–2031, Apr. 2015.

[29] I. U. Nutkani, P. C. Loh, P. Wang, and F. Blaabjerg, "Linear decentralized power sharing schemes for economic operation of ac microgrids," vol. 63, no. 1, pp. 225–234, Jan. 2016.

[30] J. M. Guerrero, L. G. de Vicuna, J. Matas, M. Castilla, and J. Miret, "Output impedance design of parallel-connected UPS inverters with wireless load-sharing control," *IEEE Trans. Ind. Electron.*, vol. 52, no. 4, pp. 1126–1135, Aug. 2005.

[31] D. A. Haughton and G. T. Heydt, "A linear state estimation formulation for smart distribution systems," *IEEE Trans. Power Syst.*, vol. 28, no. 2, pp. 1187–1195, May 2013.

[32] Y. Wang, Y. Tian, X. Wang, Z. Chen, and Y. Tan, "Kalman-filter-based state estimation for system information exchange in a multi-bus islanded microgrid," in *Proc. 7th IET Int. Conf. Power Electron., Mach. Drives (PEMD)*, Apr. 2014, pp. 1–6.

[33] Y. Wang, Z. Chen, X. Wang, Y. Tian, Y. Tan, and C. Yang, "An estimator-based distributed voltage-predictive control strategy for AC islanded microgrids," *IEEE Trans. Power Electron.*, vol. 30, no. 7, pp. 3934–3951, Jul. 2015.

[34] Q.-C. Zhong and D. Rees, "Control of uncertain LTI systems based on an uncertainty and disturbance estimator," *ASME Trans. Journal of Dyn. Sys. Meas. Con.*, vol. 126, no. 4, pp. 905–910, Dec. 2004.

[35] B. Ren, Q.-C. Zhong, and J. Chen, "Robust control for a class of non-affine nonlinear systems based on the uncertainty and disturbance estimator," *IEEE Trans. Ind. Electron.*, vol. 62, no. 9, pp. 5881–5888, Sept. 2015.

[36] B. Ren, Y. Wang, and Q.-C. Zhong, "UDE-based control of variable-speed wind turbine systems," *International Journal of Control*, vol. 90, no. 1, pp. 137–152, Jan. 2017.

[37] Y. Wang, B. Ren, and Q.-C. Zhong, "Robust power flow control of grid-connected inverters," *IEEE Trans. Ind. Electron.*, vol. 63, no. 11, pp. 6887–6897, Nov. 2016.

[38] L. Sun, D. Li, Q. C. Zhong, and K. Y. Lee, "Control of a class of industrial processes with time delay based on a modified uncertainty and disturbance estimator," *IEEE Trans. Ind. Electron.*, vol. 63, no. 11, pp. 7018–7028, Nov. 2016.

[39] R. Sanz, P. Garcia, Q. C. Zhong, and P. Albertos, "Predictor-based control of a class of time-delay systems and its application to quadrotors," *IEEE Trans. Ind. Electron.*, vol. 64, no. 1, pp. 459–469, Jan. 2017.

[40] M. Chandorkar, D. Divan, and R. Adapa, "Control of parallel connected inverters in standalone AC supply systems," *IEEE Trans. Ind. Appl.*, vol. 29, no. 1, pp. 136–143, Jan./Feb. 1993.

[41] J. C. Vasquez, J. M. Guerrero, M. Savaghebi, J. E. Garcia, and R. Teodorescu, "Modeling, analysis, and design of stationary-reference-frame droop-controlled parallel three-phase voltage source inverters," *IEEE Trans. Ind. Electron.*, vol. 60, no. 4, pp. 1271–1280, Apr. 2013.

[42] N. Pogaku, M. Prodanovic, and T. Green, "Modeling, Analysis and Testing of Autonomous Operation of an Inverter-Based Microgrid," *IEEE Trans. Power Electron.*, vol. 22, no. 2, pp. 613–625, Mar. 2007.

[43] M. J. Ryan, W. E. Brumsickle, and R. D. Lorenz, "Control topology options for single-phase UPS inverters," *IEEE Trans. Ind. Appl.*, vol. 33, no. 2, pp. 493–501, Mar./Apr. 1997.

[44] Q.-C. Zhong and D. Boroyevich, "Structural resemblance between droop controllers and phase-locked loops," *IEEE Access*, vol. 4, pp. 5733–5741, Sept. 2016.

[45] D. Swaroop, J. K. Hedrick, P. P. Yip, and J. C. Gerdes, "Dynamic surface control for a class of nonlinear systems," *IEEE Trans. Autom. Control*, vol. 45, no. 10, pp. 1893–1899, Oct. 2000.

[46] Q.-C. Zhong, G. C. Konstantopoulos, B. Ren, and M. Krstic, "Improved synchronverters with bounded frequency and voltage for smart grid integration," *IEEE Trans. Smart Grid*, 2016, DOI 10.1109/TSG.2016.2565663.

[47] J. Liu, Y. Miura, and T. Ise, "Comparison of dynamic characteristics between virtual synchronous generator and droop control in inverter-based distributed generators," *IEEE Trans. Power Electron.*, vol. 31, no. 5, pp. 3600–3611, May 2016.

[48] B. A. Francis and W. M. Wonham, "The internal model principle of control theory," *Automatica*, vol. 12, no. 5, pp. 457–465, Sept. 1976.

[49] R. Marino and P. Tomei, "Robust adaptive compensation of periodic disturbances with unknown frequency," *IEEE Trans. Autom. Control*, vol. 59, no. 10, pp. 2760–2765, Oct. 2014.

[50] B. Ren, Q.-C. Zhong, and J. Dai, "Asymptotic reference tracking and disturbance rejection of UDE-based robust control," *IEEE Trans. Ind. Electron.*, 2016, DOI 10.1109/TIE.2016.2633473.